


Quantum Lifshitz transitions generated by order from quantum disorder in strongly correlated Rashba spin-orbit-coupled systems

Fadi Sun^{1,2} and Jinwu Ye^{1,2,3}¹*Tsung-Dao Lee Institute, Shanghai 200240, China*²*Institute for Quantum Science and Engineering, Shenzhen 518055, China*³*Department of Physics and Astronomy, Mississippi State University, Mississippi State, MS 39762, USA*
 (Received 30 December 2020; revised 2 September 2021; accepted 2 September 2021; published 29 September 2021)

We study the system of strongly interacting spinor bosons in a square lattice subject to the isotropic Rashba spin-orbit coupling $\alpha = \beta$. It supports a collinear spin-bond correlated magnetic Y - x phase, a gapped coplanar in-commensurate (IC) XY - y phase, and a noncoplanar commensurate (C) 3×3 Skyrmion crystal phase. The state at the Abelian point $\alpha = \beta = \pi/2$ is just a ferromagnetic state in a rotated basis. Slightly away from the point, we identify a spurious $U(1)$ symmetry, develop a nonperturbative method to calculate not only the gap but also the excitation spectrum due to the order from quantum disorder (OFQD) mechanism. We construct a symmetry-based effective action to investigate the quantum Lifshitz transition from the Y - x state to the IC XY - y state and establish the connection between the phenomenological parameters in the effective action and those evaluated by the microscopic nonperturbative OFQD analysis in the large S limits. Experimental implications on cold atoms and some $4d$ or $5d$ Kitaev materials are discussed.

DOI: [10.1103/PhysRevA.104.L031306](https://doi.org/10.1103/PhysRevA.104.L031306)

I. INTRODUCTION

It is well-known that geometric frustrations lead to fantastic quantum, topological phases and phase transitions in quantum spin systems [1–4]. Frustrated phenomena in some typical quantum compass models such as the Kitaev honeycomb lattice model [5], 120° honeycomb lattice model [6–8], and Heisenberg-Kitaev model [9] have also been studied. On the other forefront, Rashba spin-orbit coupling (SOC) is ubiquitous in various 2D or layered noncentrosymmetric magnetic insulators, semiconductor systems, metals, and superconductors [10–17]. There have also been experimental advances in generating various kinds of 2D SOC for charge neutral cold atoms in both continuum and optical lattices [18–21]. New experimental schemes [22–26] were successfully implemented to create a long-lived SOC gas of quantum degenerate atoms. These cold atom experiments set up a very promising platform to observe many-body phenomena due to the interplay between Rashba SOC and interaction in optical lattices. It becomes important to investigate what could be the new quantum or topological phenomena due to such an interplay.

In this paper, we address this outstanding problem by studying a system of strongly interacting spinor bosons in a square lattice subject to the 2D Rashba SOC. We find that the Rashba SOC provides an alternative class of frustrated sources which leads to rich quantum phenomena even in a square lattice summarized in the abstract and Fig. 1. Our results can be applied to ongoing and near-future cold atom experiments as soon as the heating issues can be overcome in the strong coupling limit. They may also shed considerable light on the unconventional magnetic ordered states or putative quantum spin liquid states in some $4d$ or $5d$ Kitaev materials [3,4].

The tight-binding Hamiltonian of (pseudo)spin $1/2$ bosons(fermions) hopping in a two-dimensional square lattice subject to any combination of Rashba and Dresselhaus SOC is [27–30]

$$\mathcal{H}_B = -t \sum_{\langle ij \rangle} (b_{i\sigma}^\dagger U_{ij}^{\sigma\sigma'} b_{j\sigma'} + \text{H.c.}) + \frac{U}{2} \sum_i (n_i - n)^2, \quad (1)$$

where t is the hopping amplitude along the nearest neighbors $\langle ij \rangle$, n is taken to be an integer filling, $U_{ii+\hat{x}} = e^{i\alpha\sigma_x}$, $U_{ii+\hat{y}} = e^{i\beta\sigma_y}$ are the non-Abelian gauge fields put on the two links in a square lattice. $U > 0$ is the Hubbard on-site interaction.

In the strong coupling limit $U/t \gg 1$, to the order $O(t^2/U)$, we obtain the effective spin $s = n/2$ rotated ferromagnetic Heisenberg model (RFHM) [30],

$$\mathcal{H}_R = -J \sum_i [\mathbf{S}_i R(\hat{x}, 2\alpha) \mathbf{S}_{i+\hat{x}} + \mathbf{S}_i R(\hat{y}, 2\beta) \mathbf{S}_{i+\hat{y}}], \quad (2)$$

with $J = \pm 4t^2/U$ for bosons/fermions, the $R(\hat{x}, 2\alpha)$, $R(\hat{y}, 2\beta)$ are the two $SO(3)$ rotation matrices around the X and Y spin axis by angle 2α , 2β putting on the two bonds along \hat{x} , \hat{y} respectively. Expanding $U_{i,i+\hat{x}} = \cos \alpha + i \sin \alpha \sigma_x$, $U_{i,i+\hat{y}} = \cos \beta + i \sin \beta \sigma_y$ in Eq. (1), one can see that at the Abelian point $\alpha = \beta = \pi/2$, the standard hopping terms vanish, only the spin-flip hopping term (SOC) survives. As shown in Ref. [30], at the Abelian point, Eq. (2) is simply the ferromagnetic (FM) Heisenberg model in the rotated $\tilde{S}U(2)$ basis $H = -J \sum_{\langle ij \rangle} \tilde{\mathbf{S}}_i \cdot \tilde{\mathbf{S}}_j$ where $\tilde{\mathbf{S}}_i = R(\hat{x}, \pi i_x) R(\hat{y}, \pi i_y) \mathbf{S}_i$.

Both Eqs. (1) and (2) at a generic (α, β) have the translational, the time reversal \mathcal{T} , the three spin-orbital coupled Z_2 symmetries $\mathcal{P}_x, \mathcal{P}_y, \mathcal{P}_z$ symmetries [30]. Along the isotropic Rashba limit $\alpha = \beta$, the \mathcal{P}_z symmetry is enlarged to the

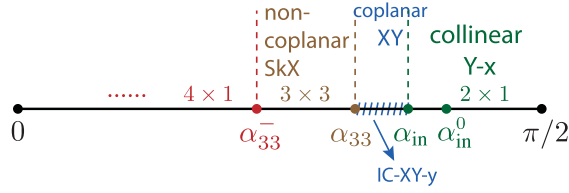


FIG. 1. The phase diagram of Eq. (2) when $\alpha = \beta^+$. The state at $\alpha = \beta = \pi/2$ is just an AFM state in $\tilde{S}\tilde{U}(2)$ basis. When $\alpha_{in} < \alpha < \pi/2$, there is a gap opening in the collinear Y - x phase generated by the order from quantum disorder (OFQD) mechanism. There is a second-order quantum Lifshitz transition (QLT) at $\alpha = \alpha_{in}$ with the dynamic exponent $z = 1$, from the Y - x phase to the coplanar IC XY - y phase [32], then a second one to the commensurate noncoplanar 3×3 SkX phase at $\alpha = \alpha_{33}$. The relevant numbers are $\alpha_{in}^0 \sim 0.3611\pi$, $\alpha_{in} \sim 0.3526\pi$, $\alpha_{33} \sim 0.3402\pi$, $\alpha_{33}^- \sim 0.295\pi$ and the ordering wave vector in the IC XY - y is $\pi - q_y^0$ with $q_{IC} \sim 0.18\pi < q_y^0 < 0.24\pi$. When $\alpha = \beta^-$. All the phases become their corresponding imaging phases related by the $[C_4 \times C_4]_D$ transformation except the 3×3 SkX phase is its own image. So, the two corresponding imaging phases can coexist with any ratio along $\alpha = \beta$.

spin-orbital coupled $[C_4 \times C_4]_D$ symmetry around the z axis. In this paper, we focus on spinor bosons with the isotropic Rashba SOC $\alpha = \beta$. The generic case $\alpha \neq \beta$ is presented in a separate publication [31].

II. THE ORDER FROM QUANTUM DISORDERS: SELECTION OF THE QUANTUM GROUND STATE

It was shown that the 2×1 (Y - x) state [30,32] is the exact quantum ground state along the anisotropic line ($\alpha = \pi/2$, $\alpha < \beta$). Now we investigate the physics along the diagonal line $\alpha = \beta$ near the Abelian point $\alpha = \beta = \pi/2$. At the classical level, the 2×1 Y - x state $S^y = (-1)^x$ [Fig. 2(a)] is degenerate with the 1×2 X - y state $S^x = (-1)^y$. In fact, due to a spurious $U(1)$ symmetry, there is a family of states called 2×2 vortex states in Fig. 2(c): $\mathbf{S}_i = ((-1)^{i_y} \cos \phi, (-1)^{i_x} \sin \phi, 0)$, which are degenerate at the classical level. The order from quantum disorder (OFQD) mechanism is needed to find the unique quantum ground state up to the $[C_4 \times C_4]_D$ symmetry in this regime. After making suitable rotations to align the spin quantization

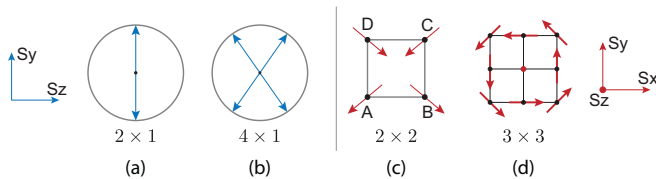


FIG. 2. The Collinear, spiral, vortex, and noncoplanar states in Fig. 1. (a) The 2×1 (Y - x) state $S^y = (-1)^x$. (b) The spin direction at the lattice sites $x = 1, 2, 3, 4$ of the 4×1 spiral state. The inset shows the spin axis for the collinear and spiral states. (c) The classically degenerate family of (two in, two out) 2×2 vortex state. (d) The 3×3 noncoplanar skyrmion crystal (SkX) state with nonvanishing skyrmion density $\vec{S}_i \cdot \vec{S}_j \times \vec{S}_k \neq 0$ happens near $\alpha = \beta = \pi/3$, which is the most frustrated regime in the Wilson loop [30]. The inset shows the spin axis for the 2×2 vortex and 3×3 SkX states.

axis along the Z axis, we introduce four Holstein-Primakoff (HP) bosons a, b, c, d corresponding to the four sublattice structures A, B, C, D shown in Fig. 2(c) to perform a systematic $1/S$ spin wave expansion [33–35] for a generic (α, β) : $H = E_0 + 2JS[H_2 + (\frac{1}{\sqrt{S}})H_3 + (\frac{1}{\sqrt{S}})^2 H_4 + \dots]$, where $E_0 = -2NJS^2(1 - \cos 2\alpha \sin^2 \phi - \cos 2\beta \cos^2 \phi)$ is the classical ground-state energy, H_n denotes the n th polynomial of the boson operators. H_2 can be diagonalized by a unitary transformation, followed by a Bogoliubov transformation as

$$H_2 = E_2 + 2 \sum_{n,k} \omega_n(k) \alpha_{n,k}^\dagger \alpha_{n,k}, \quad (3)$$

where $n = 1, 2, 3, 4$ is the sum over the four branches [due to the four sublattices A, B, C, D in Fig. 2(c)] of spin wave spectrum in the reduced Brillouin zone (BZ) $-\pi/2 < k_x, k_y < \pi/2$ and $E_2(\phi) = \sum_{k,n} [\omega_n(k) - (1 - \cos 2\alpha \sin^2 \phi - \cos 2\beta \cos^2 \phi)/2]$ is the $1/S$ quantum correction to the ground-state energy.

We first look at E_0 near the Abelian point $\alpha = \beta = \pi/2$. If $\alpha > \beta$, it picks the Y - x state [30] with $\phi = \pi/2$. If $\alpha < \beta$, it picks the X - y state with $\phi = 0$. Setting $\alpha = \beta$, $E_0 = -2NJS^2(1 - \cos 2\alpha)$ becomes ϕ independent, indicating the classical degenerate family of states characterized by the angle ϕ along the whole diagonal line $\alpha = \beta$. Fortunately, the quantum correction $E_2(\phi) = \sum_{k,n} [\omega_n(k, \phi) - \sin^2 \alpha]$ does depend on ϕ . As shown in Fig. 3(a), $E_2(\phi)$ reaches its minimum at $\phi = 0$ (X - y state) or $\phi = \pi/2$ (Y - x state), which are related to each other by the $[C_4 \times C_4]_D$ symmetry. Expanding $E_2(\phi)$ around one of its minima $\phi = 0$,

$$E_2(\phi) = E_2^0 + \frac{1}{2} B \phi^2 + \kappa \phi^4 + \dots, \quad (4)$$

where one can identify the coefficient $B(\alpha)$ plotted in Fig. 3(b). The OFQD selection of the Y - x or X - y state at $\alpha = \beta$ shows that there is a direct first-order transition from the Y - x state to the X - y state, so at $\alpha = \beta$, there is any mixture of the Y - x and X - y state in Fig. 1.

Taking the Y - x state as the ground state, plugging $\phi = \pi/2$ into Eq. (3), we find it supports the C_π magnons [30,32] at $\mathbf{k} = (0, \pi) + \mathbf{q}$. They condense along the diagonal line $\arccos(1/\sqrt{6}) \leq \alpha \leq \pi/2$ with the gapless relativistic dispersion,

$$\omega_{-0}(q) = \sqrt{v_x^2 q_x^2 + v_y^2 q_y^2}, \quad (5)$$

where $v_x = \cos(\alpha)/2$, $v_y = \cos(\alpha)\sqrt{1 - 6\cos^2(\alpha)}/2$. Obviously, both velocities vanish at the Abelian point $\alpha = \beta = \pi/2$ dictated by the hidden $\tilde{S}\tilde{U}(2)$ symmetry. Moving away from the Abelian point, v_x keeps increasing but v_y increases first, reaches a maximum, then decreases, vanishes at $\alpha_{IC}^0 = \arccos(1/\sqrt{6}) \sim 0.36614\pi$, indicating a possible quantum Lifshitz transition (QLT). As to be shown below, the gapless magnon mode in Eq. (5) is just a spurious Goldstone mode due to the spontaneous breaking of the spurious $U(1)$ symmetry.

III. ORDER FROM QUANTUM DISORDER: THE GAP OPENING AND THE SPECTRUM

By using the spin coherent state path integral formulation [1,2,33], we will evaluate the gap at the minimum $(0, \pi)$ of

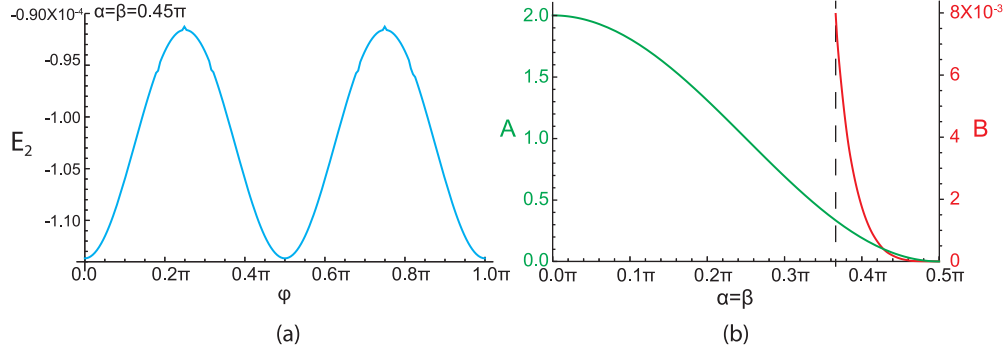


FIG. 3. The order from the quantum disorder (OFQD) and the gap opening on the spurious gapless mode in the Y - x state in Fig. 1. (a) The quantum correction $E_2(\phi)$ to the ground-state energy picks up Y - x at $\phi = 0$ or X - y at $\phi = \pi/2$ as the ground state which is related to each other by the $[C_4 \times C_4]_D$ symmetry. (b) The classical coefficient $A(\alpha)/J$ labeled by the left axis (the green line on the left) and the quantum one $B(\alpha)/J$ labeled by the right axis (the red line on the right). Both vanish at the Abelian point $\alpha = \beta = \pi/2$ as $\sim (\pi/2 - \alpha)^2$ and are monotonically increasing function when moving away from the Abelian point. The Dashed line is located at $\alpha_{in}^0 \sim 0.3661\pi$ where the Y - x state becomes unstable at the linear spin wave order. After incorporating the gap opening, the α_{in}^0 is shifted to a smaller value $\alpha_{in} \sim 0.3526\pi$. The gap Δ_B in Eq. (7) keeps increasing when moving away from the Abelian point $\alpha = \beta = \pi/2$.

the C_π magnons in the $\tilde{S}\tilde{U}(2)$ basis [30]. A general uniform state at $\vec{q} = 0$ in the $\tilde{S}\tilde{U}(2)$ basis can be taken as a FM state with the polar angle (θ, ϕ) . After transforming back to the original basis by using $\tilde{S}_1 = R_z(\pi)S_1$, $\tilde{S}_2 = R_y(\pi)S_2$, $\tilde{S}_3 = R_x(\pi)S_3$, $\tilde{S}_4 = S_4$, it leads to a 2×2 state characterized by the two angles θ and ϕ . Along the diagonal line, its classical energy becomes $H_0 = J[-2 \sin^2 \alpha - 2 \cos^2 \alpha \sin^2 \theta]$ which is, as expected, ϕ independent. Any deviation from the Abelian point picks up the XY plane with $\theta = \pi/2$. So it reduces to the 2×2 vortex state shown in Fig. 2(c). Expanding around the minimum $H_0 = J[-2 \sin^2 \alpha + 2 \cos^2 \alpha (\theta - \frac{\pi}{2})^2 + \dots]$ gives the stiffness $A = 2J \cos^2 \alpha$ shown in Fig. 3(b). Using the spin coherent state analysis, we can write down the quantum spin action at $\vec{q} = 0$,

$$\mathcal{L}(\vec{q} = 0) = iS \cos \theta \partial_\tau \phi + \frac{1}{2} S^2 A (\theta - \pi/2)^2 + \frac{1}{2} S B \phi^2, \quad (6)$$

where we put back the spin S , the first term is the spin Berry phase term, $A \sim (\pi/2 - \alpha)^2$ and $B \sim (\pi/2 - \alpha)^2$ are from the classical analysis and the OFQD analysis Eq. (4), respectively. Equation (6) leads to the gap

$$\Delta_B = \sqrt{SAB} \propto \sqrt{S}, \quad (7)$$

which is beyond any $1/S$ expansion, so nonperturbative. In fact, there are also corrections from the cubic H_3 and quartic H_4 terms in the spin wave expansion listed above Eq. (3), but they only contribute to the order of 1 which is subleading to the \sqrt{S} order in the $1/S$ expansion [33–35]. As shown in Fig. 3(b), both A and B are monotonically increasing along the diagonal line, so the gap also increases. Plugging their values at $\alpha = \alpha_{in}^0 = \arccos(1/\sqrt{6})$, taking $A/J = 1/3$, $B/J \approx 8 \times 10^{-3}$ and $S = 1/2$, we find the maximum gap near the quantum Lifshitz transition $\Delta_B/J \sim 0.036$.

In the SM1 [36], we develop a systematic nonperturbative scheme to evaluate not only the mass gap Eq. (7), but also the whole spectrum:

$$\omega_-(q_x, q_y) = \sqrt{\Delta_B^2 + v_x^2 q_x^2 + v_y^2 q_y^2 + u^2 q_y^4 + \dots} \quad (8)$$

where $v_y^2 = a(\alpha_{in}^0 - \alpha)$ changes sign at $\alpha = \alpha_{in}^0$. From the gap vanishing condition [37] (see also Eq. (10)) at the IC wavevectors $q_{IC} = \pm(\Delta_B/u)^{1/2}$, one can see the QLT is shifted to $\alpha_{IC} = \alpha_{in}^0 - 2u\Delta_B/a$. Plugging in the values of Δ_B and u , we find $q_{IC} \sim 0.18\pi$. The shift is so small that $\alpha_{ic} \sim 0.3526\pi$ remains larger than $\alpha_{33} \sim 0.3402\pi$ (to be defined in Sec. V) shown in Fig. 1. So, there must be an IC phase intervening between the Y - x state and the 3×3 state when $\alpha_{33} < \alpha < \alpha_{IC}$ in Fig. 1.

IV. THE QUANTUM LIFSHITZ TRANSITION FROM THE Y - x PHASE TO IC XY - y PHASE

Here we construct an effective action in terms of the pseudo-Goldstone mode ϕ to describe the QLT. This is a symmetry-based phenomenological approach which is independent of the $1/S$ expansion in the previous sections. Inside the Y - x phase along the diagonal line $\alpha = \beta$, after integrating out the massive conjugate variable $\theta - \pi/2$, we reach the following effective Ginzburg-Landau (GL) action in the continuum limit, consistent with all the symmetries of the microscopic Hamiltonian Eq. (2):

$$\mathcal{L}_{Y-x}[\phi] = \frac{1}{2A} (\partial_\tau \phi)^2 + v_x^2 (\partial_x \phi)^2 + v_y^2 (\partial_y \phi)^2 + u^2 (\partial_y^2 \phi)^2 + \frac{1}{2} B \phi^2 + \kappa \phi^4 + \dots \quad (9)$$

In general, it is difficult to evaluate the values of the phenomenological parameters in Eq. (9). However, in the large S limit and away from the QLT point, they can be evaluated by the microscopic calculations in the previous sections. Indeed, by contrasting Eq. (9) with Eqs. (6)–(8), one can see A is from a classical contribution, B and κ are the effective potential Eq. (4) generated from the OFQD mechanism. Notably, the coefficient $v_y^2 = a(\alpha - \alpha_{in}^0)$ tuned by the SOC changes sign at $\alpha = \alpha_{in}^0$. These matches between the microscopic calculations in a large S limit and the symmetry-based effective action ensures the nonperturbative OFQD calculation in Sec. III is indeed correct.

It is physically more transparent to rewrite Eq. (9) in the momentum space,

$$\begin{aligned} \mathcal{L}[\phi]_{Y-x,D} &= \phi(-\omega_n, -q_x, -q_y) [\omega_n^2/A + v_x^2 q_x^2 + u^2 (q_y^2 - q_{IC}^2)^2 + \Delta] \\ &\quad \times \phi(\omega_n, q_x, q_y) + \kappa \phi^4 + \dots, \end{aligned} \quad (10)$$

where $\Delta = \Delta_B^2 - \frac{a^2}{4u^2}(\alpha - \alpha_{in}^0)^2$ is the tuning parameter of the QLT.

The spin can be expressed in terms of the order parameter ϕ when using the shift $\phi \rightarrow \phi + \pi/2$ and setting ϕ small:

$$\mathbf{S}_i \sim (-(-1)^{i_y} \phi, (-1)^{i_x} \phi, 0). \quad (11)$$

So, we conclude that when $\Delta > 0$, $\langle \phi \rangle = 0$, it is inside the Y - x phase. When $\Delta < 0$, then

$$\langle \phi \rangle = P_0 \cos(q_{IC} y + \phi_0), \quad (12)$$

where P_0, ϕ_0 need to be fixed by the fourth-order κ term. Substituting it into Eq. (11) shows that the system is in the IC XY - y phase [32]. The smallness of $\langle \phi \rangle$ justifies the expansion in Eq. (4). The transition from the Y - x to the IC state is a QLT with the dynamic exponent $z = 1$. All the quantum critical scalings will be evaluated in Ref. [31] by $1/N$ expansion and $4 - \epsilon$ expansion with $\epsilon = 1$.

V. THE 3×3 NONCOPLANAR SkX PHASE

Near $\alpha = \beta = \pi/3$, it is natural to take a 3×3 ansatz, $S_{(i_x, i_y)} = S_{(i_x+3m, i_y+3n)}$, with $m, n \in \mathbb{Z}$. We estimate its classical ground-state energy by minimizing $E_{3 \times 3}(\{\phi_i, \theta_i\}_{0 \leq i \leq 9})$ over its 18 variables. Along the diagonal line ($\alpha = \beta$), as long as α is not too small, the minimization of $E_{3 \times 3}$ always leads to the 3×3 Skymion crystal (SkX) state which respects the $[C_4 \times C_4]_D$ symmetry [Fig. 2(d)]. The total spin in the 3×3 unit cell is $S_{\text{unit}} = \sum_i \mathbf{S}_i = (0, 0, 4 \times 10^{-3})$ which has exact vanishing S_x, S_y components, but still a small nonvanishing S_z component.

Comparing the classical ground energy of the 3×3 SkX with that of the Y - x state $E_{Y-x} = -2J \sin^2 \alpha$ leads to a putative first-order transition between the two states at $\alpha_{33} \approx 0.340188\pi$, which is smaller than $\alpha_{IC} \sim 0.3526\pi$ (Fig. 1). So a putative direct first-order transition between the Y - x state and the 3×3 SkX splits into two second-order QLTs with $z = 1$ with the IC XY - y phase intervening between them in Fig. 1. When approaching $\alpha = \beta$ from the anisotropic line ($\alpha = \pi/2, \beta$) from the right [31], we find $\alpha = \alpha_{33}$ lies on the constant contour line of the commensurate-incommensurate magnons $(0, k_y^0)$ at $k_y^0 \sim \pi - 0.24\pi$. So, $0.18\pi < q_y^0 < 0.24\pi$ in the IC- XY - y phase $\alpha_{33} < \alpha < \alpha_{in}$ (Fig. 1).

VI. POSSIBLE EXPERIMENTAL IMPLICATIONS

The heating issue has been well under control in the weak coupling limit in recent cold atom experiments [18–20, 22–26, 38]. So, various exotic magnetic superfluid phenomena can be observed in current cold atom experiments, however, it gets worse as the coupling increases. The RFHM Eq. (2) can only be reached in the strong coupling limit. So, the

rich magnetic Mott phenomena discovered in this paper can be observed only after the heating issue can be resolved in the strong coupling limit. Now, we turn its qualitative applications in the strongly correlated $4d$ or $5d$ materials with strong SOC.

Naively, due to its microscopic bosonic nature, the RFHM Eq. (2) may not be useful in describing the magnetism in various materials with SOC. However, the RFHM can be expanded [30] as Heisenberg-Kitaev (or compass) Dzyaloshinskii-Moriya (DM) [39] form

$$H_R = \sum_{\langle ij \rangle} J_H \vec{S}_i \cdot \vec{S}_j + \sum_{\langle ij \rangle a} J_K S_i^a S_j^a + \sum_{\langle ij \rangle a} J_D \hat{a} \cdot \vec{S}_i \times \vec{S}_j, \quad (13)$$

where $\hat{a} = \hat{x}, \hat{y}$ and $J_H = \cos 2\alpha, J_K = 2 \sin^2 \alpha, J_D = \sin 2\alpha$. One can estimate their separate numerical values near the incommensurate phase (IC XY - y) $\alpha = \alpha_{in}^0 = \arccos \frac{1}{\sqrt{6}}$ in Fig. 1: the Heisenberg term $J_H \sim -2/3$ is AFM, the Kitaev term $J_K \sim 5/3$ is FM, the DM term $J_D \sim \sqrt{5}/3$. So, the model becomes a dominant FM Kitaev term plus a small AFM Heisenberg term and a small DM term. This is indeed the case in so-called $5d$ Kitaev materials such as $A_2\text{IrO}_3$ with $A = \text{Na, Li}$ or more recent $4d$ materials $\alpha - \text{RuCl}_3$. So far, only a zigzag phase or an IC phase were observed experimentally [40, 41]; no quantum spin liquids [5, 9] have been found.

VII. DISCUSSIONS

It is instructive to contrast the quantum phenomena achieved here by the analytic perturbative and nonperturbative methods with those results achieved by classical Monte-Carlo simulations in two earlier works [28, 29]. The authors in Refs. [28, 29] did *classical* Monte Carlo simulations using the representation Eq. (13) on a small finite-size system. These two numerical papers did not have the concepts of the frustrations due to the Rashba SOC. The authors of Ref. [28] found the classical $2 \times 1, 3 \times 3$ SkX, and 4×1 states in Fig. 1. They also found a FM state near the origin $\alpha = \beta = 0$. The authors of Ref. [29] found the classical 2×2 vortex, 3×3 SkX, and 4×1 states in Fig. 1. Our paper studies the *quantum effects* on the RFHM Eq. (2) *analytically*. In Sec. II, we found the 2×2 vortex is classically degenerate with the Y - x and X - y state, but the OFQD mechanism picks up either the Y - x or X - y state as the quantum ground state. In Sec. III, we also evaluated the excitation spectrums corrected by the mechanism. This analysis also leads to the instability of the Y - x (or X - y) state to the IC SkX phase. In Sec. IV, we constructed an effective action to describe the QLT with the dynamic exponent $z = 1$ in Fig. 1 and also identified the spin-orbital structure of the IC SkX phase. Of course, it would be impossible to detect the quantum IC SkX phase by any classical Monte Carlo simulations at any finite-size system, let alone to study the QLT. Only by the controlled, nonperturbative analytical calculations, can one show there must be an incommensurate phase intervening between the collinear Y - x phase and the noncoplanar 3×3 SkX phase. Of course, the quantum model Eq. (2) presents very serious sign problem to quantum Monte Carlo simulation. So, the classical *classical* Monte-Carlo simulations used in Refs. [28, 29] cannot be extended to study the novel quantum and topological phenomena addressed in this paper.

As we alerted above, the second term in Eq. (13) is a quantum compass model in a square lattice instead of the Kitaev model in a honeycomb lattice. To have quantitative impacts on 3D or 4D Kitaev materials [40,41], it is important to extend the results achieved here in a square lattice to a honeycomb lattice with three SOC parameters α , β , γ .

ACKNOWLEDGMENTS

We thank Prof. Dapeng Yu for hospitality during our visit at Institute for Quantum Science and Engineering, and thank Prof. Wei Ku for the hospitality during our visit at the Tsung-Dao Lee Institute. We acknowledge AFOSR No. FA9550-16-1-0412 for support.

- [1] A. Auerbach, *Interacting Electrons and Quantum Magnetism*, (Springer, New York, 1994).
- [2] S. Sachdev, *Quantum Phase Transitions*, 2nd ed. (Cambridge University Press, Cambridge, 2011).
- [3] L. Savary and L. Balents, Quantum spin liquids, *Rep. Prog. Phys.* **80**, 016502 (2017).
- [4] C. Broholm, R. J. Cava, S. A. Kivelson, D. G. Nocera, M. R. Norman, and T. Senthil, Quantum spin liquids, *Science* **367**, eaay0668 (2020).
- [5] A. Kitaev, Anyons in an exactly solved model and beyond, *Ann. Phys.* **321**, 2 (2006). In the context of the present paper, the difference between honeycomb and a square lattice is not essential.
- [6] E. Zhao and W. Vincent Liu, Orbital Order in Mott Insulators of Spinless p -Band Fermions, *Phys. Rev. Lett.* **100**, 160403 (2008).
- [7] C. Wu, Orbital Ordering and Frustration of p -Band Mott Insulators, *Phys. Rev. Lett.* **100**, 200406 (2008).
- [8] H. Zou, B. Liu, E. Zhao, and W. Vincent Liu, A continuum of compass spin models on the honeycomb lattice, *New J. Phys.* **18**, 053040 (2016).
- [9] J. Chaloupka, G. Jackeli, and G. Khaliullin, Zigzag Magnetic Order in the Iridium Oxide Na_2IrO_3 , *Phys. Rev. Lett.* **110**, 097204 (2013).
- [10] Y. A. Bychkov and E. I. Rashba, Oscillatory effects and the magnetic susceptibility of carriers in inversion layers, *J. Phys. C* **17**, 6039 (1984).
- [11] J. Ye, Y. B. Kim, A. J. Millis, B. I. Shraiman, P. Majumdar, and Z. Tešanović, Berry Phase Theory of the Anomalous Hall Effect: Application to Colossal Magnetoresistance Manganites, *Phys. Rev. Lett.* **83**, 3737 (1999).
- [12] L. P. Gor'kov and E. I. Rashba, Superconducting 2D System with Lifted Spin Degeneracy: Mixed Singlet-Triplet State, *Phys. Rev. Lett.* **87**, 037004 (2001).
- [13] T. Jungwirth, Q. Niu, and A. H. MacDonald, Anomalous Hall effect in Ferromagnetic Semiconductors, *Phys. Rev. Lett.* **88**, 207208 (2002).
- [14] J. Sinova, D. Culcer, Q. Niu, N. A. Sinitsyn, T. Jungwirth, and A. H. MacDonald, Universal Intrinsic Spin Hall Effect, *Phys. Rev. Lett.* **92**, 126603 (2004).
- [15] W. Yao and Q. Niu, Berry Phase Effect on the Exciton Transport and on the Exciton Bose-Einstein Condensate, *Phys. Rev. Lett.* **101**, 106401 (2008).
- [16] N. Nagaosa, J. Sinova, S. Onoda, A. H. MacDonald, and N. P. Ong, Anomalous Hall effect, *Rev. Mod. Phys.* **82**, 1539 (2010).
- [17] J. Sinova, S. O. Valenzuela, J. Wunderlich, C. H. Back, and T. Jungwirth, Spin Hall effects, *Rev. Mod. Phys.* **87**, 1213 (2015).
- [18] L. Huang, Z. Meng, P. Wang, P. Peng, S.-L. Zhang, L. Chen, D. Li, Q. Zhou, and J. Zhang, Experimental realization of a two-dimensional synthetic spin-orbit coupling in ultracold Fermi gases, *Nat. Phys.* **12**, 540 (2016).
- [19] Z. Meng, L. Huang, P. Peng, D. Li, L. Chen, Y. Xu, C. Zhang, P. Wang, and J. Zhang, Experimental Observation of Topological Band Gap Opening in Ultracold Fermi Gases with Two-Dimensional Spin-Orbit Coupling, *Phys. Rev. Lett.* **117**, 235304 (2016).
- [20] Z. Wu, L. Zhang, W. Sun, X.-T. Xu, B.-Z. Wang, S.-C. Ji, Y. Deng, S. Chen, X.-J. Liu, and J.-W. Pan, Realization of two-dimensional spin-orbit coupling for Bose-Einstein condensates, *Science* **354**, 83 (2016).
- [21] Z.-Y. Wang, X.-C. Cheng, B.-Z. Wang, J.-Y. Zhang, Y.-H. Lu, C.-R. Yi, S. Niu, Y. Deng, X.-J. Liu, S. Chen, and J.-W. Pan, Realization of an ideal Weyl semimetal band in a quantum gas with 3D spin-orbit coupling, *Science* **372**, 271 (2021).
- [22] M. L. Wall, A. P. Koller, S. Li, X. Zhang, N. R. Cooper, J. Ye, and A. M. Rey, Synthetic Spin-Orbit Coupling in an Optical Lattice Clock, *Phys. Rev. Lett.* **116**, 035301 (2016).
- [23] L. F. Livi, G. Cappellini, M. Diem, L. Franchi, C. Clivati, M. Frittelli, F. Levi, D. Calonico, J. Catani, M. Inguscio, and L. Fallani, Synthetic Dimensions and Spin-Orbit Coupling with an Optical Clock Transition, *Phys. Rev. Lett.* **117**, 220401 (2016).
- [24] S. Kolkowitz, S. L. Bromley, T. Bothwell, M. L. Wall, G. E. Marti, A. P. Koller, X. Zhang, A. M. Rey, and J. Ye, Spin-orbit coupled fermions in an optical lattice clock, *Nature* **542**, 66 (2017).
- [25] F. A. An, E. J. Meier, and B. Gadway, Direct observation of chiral currents and magnetic reflection in atomic flux lattices, *Sci. Adv.* **3**, e1602685 (2017).
- [26] N. Q. Burdick, Y. Tang, and B. L. Lev, Long-lived spin-orbit-coupled degenerate dipolar Fermi gas, *Phys. Rev. X* **6**, 031022 (2016).
- [27] Z. Cai, X. Zhou, and C. Wu, Magnetic phases of bosons with synthetic spin-orbit coupling in optical lattices, *Phys. Rev. A* **85**, 061605(R) (2012).
- [28] J. Radić, A. Di Ciolo, K. Sun, and V. Galitski, Exotic Quantum Spin Models in Spin-Orbit-Coupled Mott Insulators, *Phys. Rev. Lett.* **109**, 085303 (2012);
- [29] W. S. Cole, S. Zhang, A. Paramekanti, and N. Trivedi, Bose-Hubbard Models with Synthetic Spin-Orbit Coupling: Mott Insulators, Spin Textures, and Superfluidity, *Phys. Rev. Lett.* **109**, 085302 (2012).
- [30] F. Sun, J. Ye, and W.-M. Liu, Quantum magnetism of spinor bosons in optical lattices with synthetic non-Abelian gauge fields, *Phys. Rev. A* **92**, 043609 (2015).
- [31] F. Sun and J. Ye, Two classes of organization principle: Quantum/topological phase transitions meet complete/incomplete devil staircases and their experimental realizations, [arXiv:1603.00451](https://arxiv.org/abs/1603.00451).

- [32] Here we still use the same notation used in Ref. [30]. In the $Y-(\pi, 0)$ called $Y-x$ state, the first letter indicates the spin polarization, the second letter indicates the $(\pi, 0)$ orbital order. Along the anisotropic line ($\alpha = \pi/2, \beta$), it supports three kinds of magnons C_0 , IC, and C_π with their minimum at $(0, 0)$, $(0, \pm k_y^0)$ and $(0, \pi)$, respectively. The IC-XY-y phase means IC in the spin XY plane with the IC momentum along the y axis.
- [33] G. Murthy, D. Arovas, and A. Auerbach, Superfluids and superfluids on frustrated two-dimensional lattices, *Phys. Rev. B* **55**, 3104 (1997).
- [34] R. T. Scalettar, G. G. Batrouni, A. P. Kampf, and G. T. Zimanyi, Simultaneous diagonal and off-diagonal order in the Bose-Hubbard Hamiltonian, *Phys. Rev. B* **51**, 8467 (1995).
- [35] Jun-ichi Igarashi, $1/S$ expansion for thermodynamic quantities in a two-dimensional Heisenberg antiferromagnet at zero temperature, *Phys. Rev. B* **46**, 10763 (1992); Jun-ichi Igarashi and T. Nagao, $1/S$ -expansion study of spin waves in a two-dimensional Heisenberg antiferromagnet, *ibid.* **72**, 014403 (2005).
- [36] See Supplemental Material at <http://link.aps.org/supplemental/10.1103/PhysRevA.104.L031306> for the derivation of the complete excitation spectrum Eq. (8) due to the OFQD phenomena.
- [37] L. Jiang and J. Ye, Lattice structures of Larkin-Ovchinnikov-Fulde - Ferrell (LOFF) state, *Phys. Rev. B* **76**, 184104 (2007).
- [38] M. Gong, Y. Qian, M. Yan, V. W. Scarola, and C. Zhang, Dzyaloshinskii-Moriya interaction and spiral order in spin-orbit coupled optical lattices, *Sci. Rep.* **5**, 10050 (2015).
- [39] I. Dzyaloshinskii, A thermodynamic theory of “weak” ferromagnetism of antiferromagnetics, *J. Phys. Chem. Solids* **4**, 241 (1958); T. Moriya, Anisotropic superexchange interaction and weak ferromagnetism, *Phys. Rev.* **120**, 91 (1960).
- [40] A. Biffin, R. D. Johnson, I. Kimchi, R. Morris, A. Bombardi, J. G. Analytis, A. Vishwanath, and R. Coldea, Noncoplanar and Counterrotating Incommensurate Magnetic Order Stabilized by Kitaev Interactions in γ -Li₂IrO₃, *Phys. Rev. Lett.* **113**, 197201 (2014).
- [41] A. Biffin, R. D. Johnson, S. Choi, F. Freund, S. Manni, A. Bombardi, P. Manuel, P. Gegenwart, and R. Coldea, Unconventional magnetic order on the hyperhoneycomb Kitaev lattice in Li₂IrO₃: Full solution via magnetic resonant x-ray diffraction, *Phys. Rev. B* **90**, 205116 (2014).